

# Re-entrant melting and freezing in a model system of charged colloids

C. Patrick Royall<sup>a)</sup>*Institute of Industrial Science, University of Tokyo, Komaba 4-6-1, Meguro-ku, Tokyo 153-8505, Japan*

Mirjam E. Leunissen

*Soft Condensed Matter, Debye Institute, Utrecht University, Princetonplein 5, 3584 CC Utrecht, The Netherlands*

Antti-Pekka Hynninen

*Department of Chemical Engineering, Princeton University, Princeton New Jersey 08544-5263*

Marjolein Dijkstra and Alfons van Blaaderen

*Soft Condensed Matter, Debye Institute, Utrecht University, Princetonplein 5, 3584 CC Utrecht, The Netherlands*

(Received 24 October 2005; accepted 28 February 2006; published online 28 June 2006)

We studied the phase behavior of charged and sterically stabilized colloids using confocal microscopy in a low polarity solvent (dielectric constant 5.4). Upon increasing the colloid volume fraction we found a transition from a fluid to a body centered cubic crystal at  $0.0415 \pm 0.0005$ , followed by reentrant melting at  $0.1165 \pm 0.0015$ . A second crystal of different symmetry, random hexagonal close packed, was formed at a volume fraction around 0.5, similar to that of hard spheres. We attribute the intriguing phase behavior to the particle interactions that depend strongly on volume fraction, mainly due to the changes in the colloid charge. In this low polarity system the colloids acquire charge through ion adsorption. The low ionic strength leads to fewer ions per colloid at elevated volume fractions and consequently a density-dependent colloid charge. © 2006 American Institute of Physics. [DOI: 10.1063/1.2189850]

## I. INTRODUCTION

Freezing and melting are common everyday physical phenomena. More unusual is the reentrant melting, which usually stems from a subtle interplay between enthalpy and entropy, and may be found in systems as diverse as discotic liquid crystals,<sup>1</sup> diblock copolymer solutions,<sup>2</sup> and helium 3.<sup>3</sup> We present results on a model system of charge-stabilized colloids, which exhibits an intriguing reentrant colloidal fluid phase at a higher volume fraction than a colloidal crystal, and a second crystal phase with different symmetry at a higher volume fraction still. The phase behavior of colloids dispersed in a solvent is thermodynamically equivalent to that of atoms and small molecules,<sup>4,5</sup> however, colloids can be studied with optical microscopy due to their relatively large size. We analyzed the structure in three-dimensional (3D) real space, at the single particle level using confocal laser scanning microscopy (CLSM).<sup>6</sup>

Under many circumstances, the biologically and industrially relevant system of charged colloids is described by a screened Coulomb (“Yukawa”) interaction.<sup>7-9</sup> In this work we will neglect the Van der Waals attractions, since they are reduced to a fraction of the thermal energy by matching the refractive index of the colloids and the solvent.<sup>5</sup> A linearization of the mean-field Poisson-Boltzmann theory used by Derjaguin, Landau, Verwey, and Overbeek,<sup>7</sup> combined with a hard-core term due to the physical size of the colloids, describes the interaction between two colloids with constant surface potential as

$$\beta u(r) = \begin{cases} \infty, & r \leq \sigma \\ \frac{Z^2}{(1 + \kappa\sigma/2)^2} \frac{l_B \exp(-\kappa(r - \sigma))}{\sigma r/\sigma}, & r > \sigma, \end{cases} \quad (1)$$

where  $\beta = 1/k_B T$ ,  $Z$  is the number of charges on a colloid,  $\sigma$  is the colloid diameter,  $r$  is the center-to-center separation,  $k_B$  is Boltzmann’s constant, and  $T$  is the absolute temperature. The Bjerrum length of the solvent is given by  $l_B = \beta e^2 / \epsilon_S$  where  $e$  is the elementary charge and  $\epsilon_S$  is the permittivity. The inverse Debye screening length is denoted by  $\kappa = \sqrt{4\pi l_B \rho_i}$  where  $\rho_i$  is the total number density of monovalent ions. These ions have several sources, “background” ions, due to solvent self-dissociation and impurities, and counterions which balance the charge on the colloids.

Often the parameters used in Eq. (1) are taken to be constant with respect to volume fraction. In earlier work we found this to be a good approximation.<sup>10</sup> However, as we shall discuss in this paper, the colloid charge and Debye length can be a function of volume fraction for a variety of reasons. The linear Poisson-Boltzmann theory assumed in Eq. (1) is only valid for small electrostatic potentials (colloid charges). However, at higher potentials, the pair interaction can still be described as Yukawa-type, but with a smaller, renormalized charge, except for very small separations.<sup>8</sup> Charge renormalization leads to volume fraction dependent interactions.<sup>11</sup> Renormalization has successfully been used to compare experimental phase behavior to the Yukawa potential,<sup>12</sup> but did not explain the reentrant fluid formed by increasing the colloid charge at constant volume fraction.<sup>13</sup> In addition, when the counterions form a significant fraction

<sup>a)</sup>Electronic mail: paddy@iis.u-tokyo.ac.jp

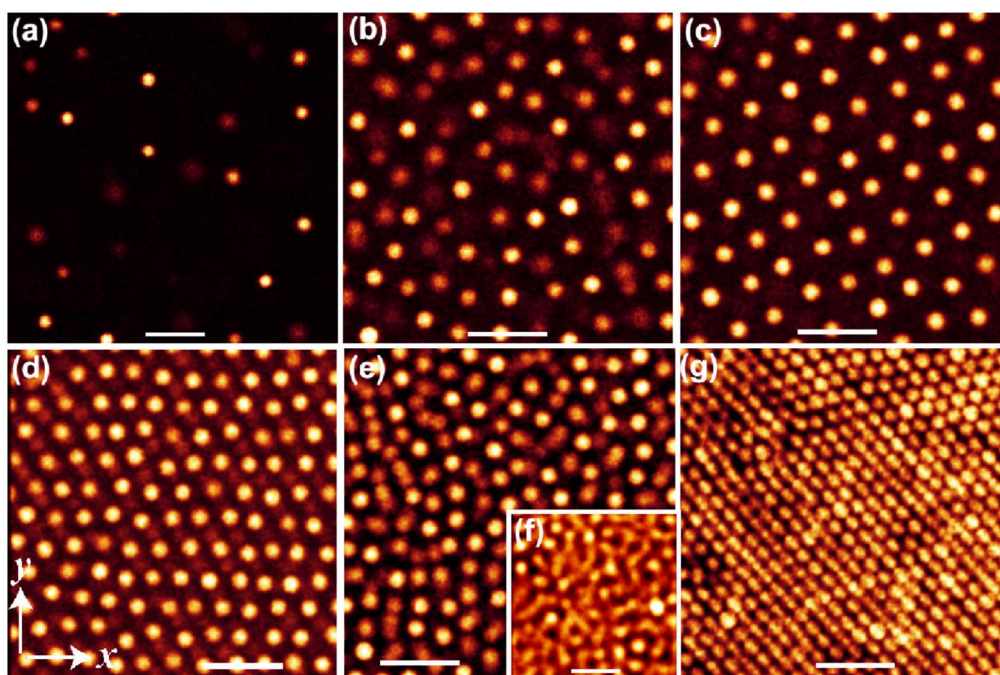


FIG. 1. Confocal microscopy images of phase behavior as a function of volume fraction,  $h$ . Initially, a fluid is seen, [(a)  $h=0.0037$ , (b)  $h=0.041$ ], forming a BCC crystal [(c)  $h=0.042$ , (d)  $h=0.115$ ]. What is unusual is the reentrant fluid [(e), (f)  $h=0.118$ ]. Finally, a RHCP crystal is formed [(g), (h) 0.5]. A time-lapse over 4 min, indicating homogeneous diffusion is shown in (f). All other images are single  $xy$  scans of 500 ms duration. Bars=10  $\mu\text{m}$ .

of the ionic strength, the colloid-colloid interactions depend strongly on the volume fraction, decreasing the volume fraction reduces the ionic strength, increases the Debye length and can enhance the structure at low densities.<sup>14</sup>

Moreover, when the range of the interaction exceeds the mean interparticle separation, the assumption of pairwise additivity becomes questionable.<sup>15,16</sup> Effective attractions due to nonpairwise additivity<sup>17,18</sup> may help explain a range of recent experimental observations such as superheated crystals,<sup>19</sup> and “liquid-gas” phase separation,<sup>20</sup> which are not expected for purely repulsive interactions. Attractions can also be caused by correlations between small ions.<sup>21</sup> Volume fraction dependent attractions may also explain reentrant phase behavior, so in addition to simulations using Eq. (1), we compared our results to the primitive model. Nonpairwise additivity and correlations are included in the primitive model, where all charged species, including the small ions, interact via a Coulomb potential with a hard core,

$$\beta u(r) = \begin{cases} \infty, & r < \frac{1}{2}(\sigma_i + \sigma_j) \\ \frac{q_i q_j l_B}{r}, & r \geq \frac{1}{2}(\sigma_i + \sigma_j), \end{cases} \quad (2)$$

where  $i$  and  $j$  are the interacting species, and may be colloids ( $q=Z$ ) or monovalent co- or counterions ( $q=1$ ) and  $\sigma_{ij}$  is the diameter.<sup>22,23</sup>

Here we studied the phase behavior of a suspension of charged and sterically stabilized poly-methyl methacrylate (PMMA) colloids in a (almost) index and density matching solvent mixture with a dielectric constant of 5.4.<sup>24</sup> Upon increasing the volume fraction, we found a colloidal fluid, followed by a body centered cubic (BCC) crystal, which melted to a reentrant fluid and then a second freezing

transition to a crystal of different symmetry, random hexagonal close packed (RHCP) (Fig. 1). By contrast, the phase diagram for Yukawa systems [Eq. (1)] exhibits only one fluid-crystal transition, as a function of colloid concentration.<sup>34</sup> The reentrant melting observed here may be reconciled with the Yukawa interaction only by allowing the colloid charge and Debye screening length to vary as a function of volume fraction. In other words, the Yukawa interaction is density dependent. By comparing the results of experiments with Monte Carlo (MC) simulations, we can obtain an estimate of the colloid charge and Debye length as a function of volume fraction. We also made independent measurements of the colloid charge in dilute dispersions with electrophoresis. The work reported here contrasts with the previous measurements on a similar system,<sup>10</sup> in which we found a fixed pair potential as a function of colloid volume fraction. We highlight the differences between these experiments below. This paper is organized as follows: first, we describe our experimental and simulation methods, followed by results. Our discussion identifies the possible causes for the unusual phase behavior observed.

## II. EXPERIMENT

We used the sterically stabilized, poly-methyl methacrylate colloids of 2.16  $\mu\text{m}$  diameter in a solvent mixture of *cis*-decalin and cyclohexyl bromide (CHB). By closely matching both the refractive index and mass density of the colloids,<sup>24</sup> the system is optimized for optical techniques. The colloids were labeled with rhodamine isothiocyanate<sup>25</sup> but we saw a similar behavior using colloids labeled with 7-nitrobenzo-2-oxa-1,3-diazol, and conclude that the dye has little influence. We purified the CHB solvent by washing and distilling as described previously.<sup>10</sup> The dielectric constant of

the solvent mixture was 5.37, determined with dielectric spectroscopy.<sup>26</sup> The dispersions were confined to glass capillaries with inner dimensions of  $0.1 \times 1.0 \text{ mm}^2$  (VitroCom) and sealed at each end with Norland Optical adhesive no. 68 (Norland Optical Products Inc). We checked that melt sealing the glass gave the same behavior. In a typical experiment the dispersion had an initial volume fraction of 0.04 and was centrifuged at 1000 rpm (Hettich Zentrifugeren Rontina 46s) for 18 h to create a concentration gradient, and then lay horizontally for 24 h to allow the small ions to equilibrate. After sedimentation we found that around 90% of the capillary was free from colloids, and functioned as an ion reservoir.

To reveal the phase behavior we scanned the gradient in colloid concentration resulting from the centrifugation using a Leica SP2 CLSM with a  $63\times$  NA 1.4 oil immersion objective, in fluorescence mode with 543 nm excitation. The images were taken at least  $20 \mu\text{m}$  from the capillary wall. Charged colloids in a gravitational or centrifugal field can setup a macroscopic electric field,<sup>27</sup> but the impact of this electric field on the pair interactions is negligible for our range of parameters.<sup>28</sup> Similarly, the effect of gravity is small here, since the gravitational height is around  $100 \mu\text{m}$ , which is comparable to the thickness of the glass capillary in which the samples were confined. We stress that, although the system is, in principle, in a metastable state due to the concentration gradient, the diffusion of  $2.16 \mu\text{m}$  diameter colloids is sufficiently slow that the gradient, which typically spanned a few millimeters, was still present after months. Certainly, no local change in colloid volume fraction and structure was found during data acquisition (up to 3 h). Although the colloid concentration gradient may be regarded as fixed, the small ion concentration is expected to relax after a few hours, on a centimeter length scale. We present the results from concentration gradient samples in equilibrium with an ion reservoir, but also prepared a number of separate samples at differing volume fractions, and saw similar behavior, giving strong evidence that our observations are not due to the metastable density profile induced in the colloids by centrifugation.

We analyzed the structure of the colloidal suspension to obtain a value for the colloid charge. Other, more direct methods may also be used, in principle, such as titration, electrophoresis and electroacoustic, characterization. However, these techniques do not necessarily determine the effective charge that governs the experimental phase behavior. For instance, titration measures the bare charge, which is not relevant here. The electrokinetic techniques have another drawback, their theoretical interpretation at higher volume fractions is not sufficiently developed at this time. However, we have performed electrophoresis measurements on dilute ( $\eta=0.0015$ ) samples. We made the measurements with a Coulter Delsa 440SX and determined the stationary layers from Komagata linearization. We used the Hückel equation to relate the mobility to the zeta potential and used the empirical relationship proposed by Loeb *et al.* to determine the zeta potential from the colloid charge.<sup>29</sup> We assumed that the zeta potential is the actual surface potential, which is appropriate in the case of small surface charge and long Debye length, as is the case here. We also made conductivity mea-

surements using a variety of solvent batches and colloid concentrations, using a Scientifica 627 conductivity meter, in order to study the origin of the reentrant melting behavior.

### III. ANALYSIS: DETERMINING THE COLLOID CHARGE AND DEBYE SCREENING LENGTH

Central to this work is the extraction of the colloidal interactions from confocal microscopy data. We consider two strategies, for colloidal fluids and crystals, respectively. In the case of fluids, a measurement of the radial distribution function  $g(r)$  can be used to determine the pair interaction. We found that the assumption of pairwise additivity is indeed a sufficient description of this system. In principle, the interaction potential is uniquely determined by the  $g(r)$  for pairwise additive systems,<sup>30</sup> and may be extracted by inversion techniques.<sup>31</sup> However, such methods require a radial distribution function of higher precision than that which we can measure here in 3D [the details of our method to determine  $g(r)$  are given in Ref. 10]. We therefore assumed that the colloidal interactions have a Yukawa form [Eq. (1)]. We carried out the MC simulations in the canonical ensemble<sup>32</sup> with various combinations of the colloid charge  $Z$ , and the Debye screening length  $\kappa^{-1}$  and compared the resulting  $g(r)$ 's with the experimental data. We selected those which gave the best agreement and assumed the input parameters to the simulation were the same as those in the experiment. However, due to the error in the measured radial distribution functions, there was some variation in the simulation input parameters which gave good agreement, thus there is an uncertainty in the values we obtained for the colloid charge and Debye length, which depends on the state point. This uncertainty is estimated as 20% in both  $Z$  and  $\kappa^{-1}$  for the dilute fluid phase, and 20% in  $Z$  and 40% in  $\kappa^{-1}$  for the reentrant fluid phase. In every experiment, the values of  $Z$  and  $\kappa^{-1}$  were corresponded to a fluid according to Eq. (1).

We extended our analysis to address some of the assumptions of Eq. (1). In particular, the restrictions of the linear Poisson-Boltzmann theory and pairwise additivity between the colloids are lifted in the primitive model [Eq. (2)]. The primitive model also includes effects of ion correlations, although these are extremely small in this system. In the primitive model simulations, we again varied the colloid charge and Debye length and compared the results both to the Yukawa interaction [Eq. (1)] and experiment. Here the primitive model is implemented on a lattice, where the lattice spacing is chosen so each colloid diameter is divided into 19 lattice sites.<sup>23</sup> We found that different sized lattices gave indistinguishable  $g(r)$ 's for our parameters, and concluded that the lattice discretization had no effect on our results.

In the colloidal crystal, the particles are confined to a potential well formed by the interactions with their neighbors,  $w(d)$ , where  $d$  is the displacement from the lattice site. For displacements less than 10% of the interparticle separation, the well is approximately harmonic, so  $\beta w(d) \sim \alpha d^2/2$  with  $\alpha$  the "effective spring constant," as shown in Fig. 2.<sup>33</sup> To calculate  $\alpha$ , we sample typically 500 configurations of around 400 particles. The mean position of each particle is determined, and the excursions are measured, from which we

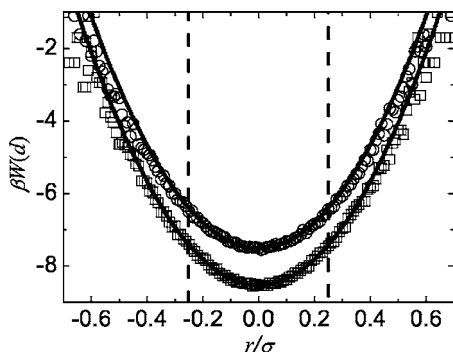


FIG. 2. Particle displacement from mean lattice position, for  $h=0.103$ . Squares and circles are experimental  $x$  and  $y$  data, respectively.  $x$  and  $y$  are defined in Fig. 1(d). Solid lines are quadratic fits that are taken between the dotted lines to yield the ‘effective spring constant’,  $a$ . Data offset for clarity.

calculate the likelihood of an excursion of given distance. The logarithm of the likelihood then gives the potential well, which we fit to a quadratic form for less than 10% of the interparticle separation (Fig. 2). In exactly the same way, we can also calculate  $\alpha$  from simulation data. Thus, given a trial pair interaction, we can compare the results of simulated and experimental effective spring constants, in a conceptually similar way to the  $g(r)$  method above. However, since we compare only a scalar, fitting a two-parameter potential such as Eq. (1) is not possible. We can, however, identify whether a given input potential gives good agreement with the experimental data. Note that the direct comparison with melting measures such as the Lindemann criterion is difficult: the limited sample size leads to an overestimation of the  $\alpha$  values. However, the system sizes for experiment and simulation data were kept very similar, and the identical analysis leads to a robust comparison.

#### IV. RESULTS

Previously, we found a fluid to face centered cubic crystal phase transition at a colloid volume fraction of  $\eta \approx 0.1$ .<sup>10</sup> Both the phase transition and the fluid structure were consistent with a density independent Yukawa potential [Eq. (1)] (Ref. 34) with a colloid charge around 600 and Debye screening length of 400 nm. Those results contrast strongly with the behavior shown in Fig. 1 which forms the subject of this article. For  $\eta \leq 0.041$ , a colloidal fluid is seen [Figs. 1(a) and 1(b)], whose long-ranged repulsions are suggested by the considerable separation between the particles in Fig. 1(a) [see also Fig. 3(a), bottom line]. Upon compression this fluid forms a BCC crystal at  $\eta = 0.0415 \pm 0.0005$  [Fig. 1(c)]. What is unusual is that the crystal melts, at  $\eta = 0.1165 \pm 0.0015$  [Figs. 1(d) and 1(e)] into a reentrant fluid [Fig. 1(e)], with completely isotropic diffusion of the particles [Fig. 1(f)]. There is a second crystallization, to an RHCP structure, at  $\eta \approx 0.50$ , [Fig. 1(g)]. This second crystallization cannot be distinguished from that reported for hard spheres,<sup>4</sup> although the colloids still carry some charge.<sup>34</sup>

Figure 3 shows experimental radial distribution functions and the results from the Yukawa potential and primitive model simulations. In the low volume fraction fluid [Fig. 3(a)], we fitted the  $g(r)$ s with a modest decrease in charge

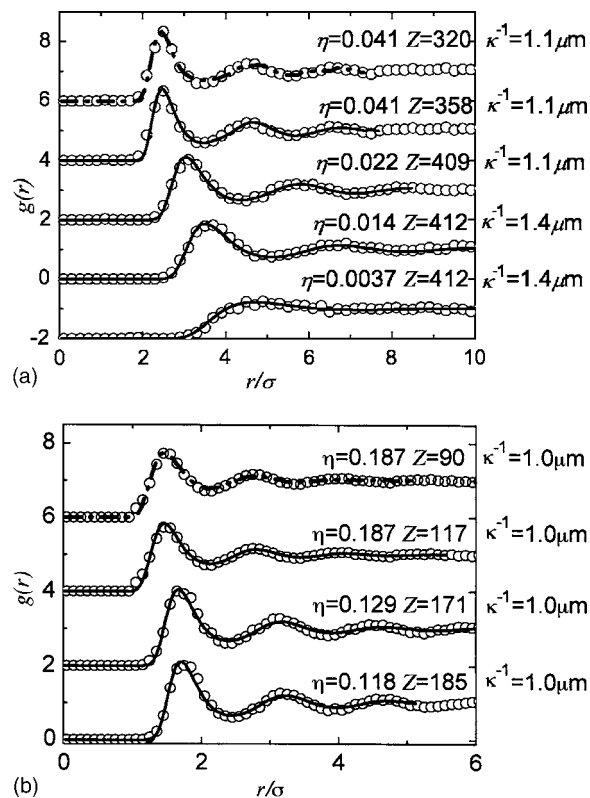


FIG. 3. The radial distribution function at various colloid volume fractions in the low volume fraction fluid (a) and reentrant fluid (b). Circles are experimental data. MC simulation data for the Yukawa potential (solid lines) and primitive model (top, dashed) are also plotted. Data offset for clarity.

from  $Z=412$  to  $Z=358$  from  $\eta=0.0037$  to  $0.041$ . The charge reduction in the reentrant fluid is rather greater, to 185 by  $\eta=0.118$  and 117 by  $\eta=0.187$  [Fig. 3(b)]. In the low volume fraction fluid ( $\eta \leq 0.041$ ), the Debye length fell from  $1.4 \pm 0.3$  to  $1.1 \pm 0.2 \mu\text{m}$ , while in the reentrant fluid,  $g(r)$  fitting suggests  $\kappa^{-1} = 1.0 \pm 0.4 \mu\text{m}$ . These values are consistent with ions in a colloidal suspension in ‘Donnan’ equilibrium with an ion reservoir with  $\kappa^{-1} = 1.5 \mu\text{m}$  at the colloid charge and volume fraction measured. The results from the primitive model have the same trend of a charge which falls with volume fraction, but the values are slightly lower,  $Z=320$  and  $90$  for  $\eta=0.041$  and  $0.187$ , respectively, in line with nonlinear Poisson-Boltzmann results.<sup>9</sup> Since the primitive model, which includes a nonpairwise additivity and is not restricted to the linear Poisson-Boltzmann regime, gives similar values to the Yukawa interaction, we conclude that neither of these effects matter greatly for our parameters. Within the scope of this work, the pairwise Yukawa interaction [Eq. (1)] thus provides a satisfactory description. Although the reduction in charge is consistent with a reentrant fluid, on the basis of the phase behavior alone we cannot exclude the possibility of a reentrant fluid phase in the presence of a constant colloid charge: if the Debye length were to fall sufficiently, then a Yukawa model could predict a reentrant melting as well.<sup>34</sup> However, in this case, a threefold fall in the Debye length is needed in the range  $\eta = 0.0415 \pm 0.0005 - \eta = 0.1165 \pm 0.0015$ , corresponding to an unphysical order of magnitude increase in ionic strength. We have also measured the conductivity as a function of colloid

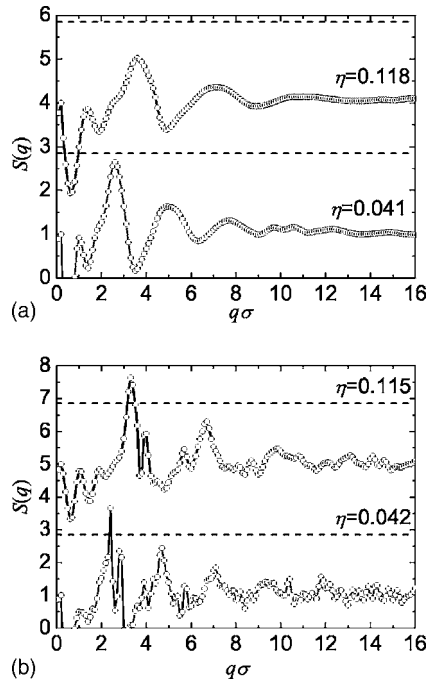


FIG. 4. The static structure factor  $S(q)$  close to freezing. The low-density fluid (a), bottom data, reentrant fluid (a), top data, and BCC crystal. (b) are compared with the Hansen-Verlet melting criterion,  $S(q_p)=2.85$  (dashed lines). The minima at low  $q$  are artifacts of the Fourier transform. Data offset for clarity.

volume fraction, and find no large increase in conductivity, further supporting our analysis of the confocal microscopy data. We can also Fourier transform  $g(r)$  to the static structure factor  $S(q)$ , where  $q$  is the wave vector. Such structure factors are shown in Fig. 4(a), for fluids  $\eta=0.041$  and  $\eta=0.118$ , those statepoints which lie closest to the BCC phase. The Hansen-Verlet criterion identifies the height of the first peak of the structure factor,  $S_p(q_p)$ , as around 2.85 at melting.<sup>35</sup> The first peaks in both structure factors in Fig. 4(a) are lower than 2.85, and are thus consistent with the Hansen-Verlet criterion for equilibrium fluids. Furthermore we calculated the structure factors of the BCC crystal phase. In this case, it was hard to acquire 3D images over a sufficient lengthscale, so we used two-dimensional (2D) data. The results are shown in Fig. 4(b), for  $\eta=0.042$  and 0.115. In both cases, the first peak exceeds 2.85, so we conclude that our results are fully compatible with the Hansen-Verlet criterion.

The decrease in colloid charge with volume fraction is shown in Fig. 5. Unfilled circles are obtained from  $g(r)$  fits with the Yukawa potential, while triangles are primitive model results. In the BCC phase, we were able to estimate the Debye length by interpolating between the values at the highest density in the dilute fluid phase ( $\eta=0.041$  and  $\kappa^{-1}=1.1 \mu\text{m}$ ) and the lowest density in the reentrant fluid phase ( $\eta=0.118$  and  $\kappa^{-1}=1.0 \mu\text{m}$ ). In order to determine the colloid charge, we further assumed sufficiently strong interactions for crystallization according to Eq. (1)<sup>34</sup> This provided a lower bound to the colloid charge. As mentioned above, in the BCC phase, we determined an effective spring constant  $\alpha$ . For these parameters, the potential well which confines each particle is almost spherically symmetric. Consequently,

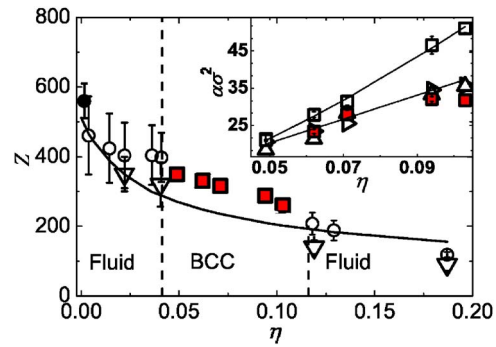


FIG. 5. Colloid charge  $Z$  plotted as a function of volume fraction,  $h$ , as found from electrophoresis (filled circle),  $g(r)$  fitting with the Yukawa potential (unfilled circles) and primitive model (triangles). The filled squares denote the charge estimated from the Yukawa phase diagram (Ref. 34) (filled squares). Solid line is a guide to the eye. Dashed lines are approximate phase boundaries. Inset: Effective spring constant  $k$ . Triangles are experimental data. Filled squares correspond to simulation using estimated charge in main figure, unfilled squares to constant charge.

similar values of  $\alpha_x$  (triangle right), and  $\alpha_y$  (triangle up) (Fig. 5, inset) were obtained. The directions  $x$  and  $y$  are defined by the orientation in Fig. 1(d). We also determined  $\alpha$  from the Yukawa potential MC simulations, using the values we estimated above for the charge in the BCC crystal phase (Fig. 5, filled squares). The simulated  $\alpha$  values are shown as filled squares in the inset of Fig. 5. The agreement with the experimental data is good. For comparison, we also assumed a constant charge of  $Z=358$  (Fig. 5 inset, unfilled squares). In this constant charge case,  $\alpha$  increases as a function of volume fraction significantly faster than the experimental measurements. Figure 5 (inset) shows that in the colloidal crystal too, the charge appears to decrease. We also show the results of electrophoresis measurements,  $Z=560 \pm 50$ , (Fig. 5, filled circle). This provides an independent check of the colloid charge at low volume fractions which is consistent with our analysis of the confocal microscopy data.

The Yukawa systems with arbitrary Debye lengths, volume fractions and colloid charges may be plotted on a single set of axes in the  $(\lambda, \tilde{T})$  (Ref. 36) representation, where  $\lambda$  is a scaled Debye length and  $\tilde{T}$  is an effective temperature. Furthermore, in this representation, the phase boundaries are almost straight lines.<sup>37</sup> Although the  $(\lambda, \tilde{T})$  representation only applies to point Yukawa particles, it turns out that, for the parameters considered here, the hard core has negligible effect on the phase behavior for  $\eta=0.187$ .<sup>34</sup> We therefore ignore the hard core, and map the parameters of our statepoints obtained from fitting the experimental data with a Yukawa interaction to  $(\lambda, \tilde{T})$  as follows:

$$\lambda = \kappa\sigma(6\eta/\pi)^{-1/3}, \quad (3)$$

$$\tilde{T} = \left[ \frac{2}{3}\lambda^2\beta u_M(\lambda) \right]^{-1}, \quad (4)$$

where  $u_M$  is the Madelung energy per particle in an ideal face-centered cubic (FCC) crystal.<sup>34</sup> Figure 6 shows the statepoints of the reentrant system that is the subject of this article (unfilled symbols) and the previous statepoints which did not show any reentrant melting (filled symbols).<sup>10</sup> The nonreentrant system takes only a slightly curved path as the

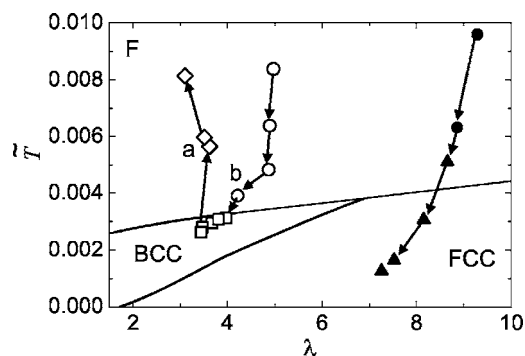


FIG. 6. Phase diagram in the  $(\lambda, \tilde{T})$  representation (see text). The arrows denote increasing colloid volume fraction. Filled symbols are earlier experimental statepoints (Ref. 10), fluid and FCC crystal phases are represented by circles and triangles, respectively. The unfilled circles, squares, and diamonds correspond to experimental statepoints in the low-density fluid, BCC crystal, and reentrant fluid. The higher density RHCP crystal is not shown in this representation. (a) and (b) represent those statepoints for which  $S(q)$  was calculated,  $h=0.118$  and  $h=0.041$ , respectively.

colloid volume fraction is increased, as indicated by the arrows. Since the melting line is approximately straight in Fig. 6, in order to cross the line twice (reentrant melting), the path in the  $(\lambda, \tilde{T})$  representation must exhibit a return. The fluid statepoints for which we calculated  $S(q)$  in Fig. 4(a) are shown in Fig. 6 as **a** and **b** for  $\eta=0.118$  and  $0.041$ , respectively. Note that point **a** lies rather further from the melting line than does point **b**, consistent with the lower value of the peak in  $S(q)$ . Our experimental statepoints show good agreement with the phase diagram of point Yukawa particles.

## V. CONDUCTIVITY MEASUREMENTS

Above, we have argued that the colloid interactions depend strongly on volume fraction. In particular, both the primitive model and Yukawa potential show that the colloid charge appears to decrease with volume fraction. This fall is too large to be explained by assuming a constant surface potential, rather than constant charge.<sup>7</sup>

The exact nature of the charging process in the solvent mixture is not yet fully understood, so providing a complete explanation of the fall in colloid charge is difficult. Here we present some observations that may guide towards an understanding of the chemistry underlying the unusual phase behavior observed. We begin by summarising our observations. We have studied four systems of PMMA in the CHB-decalin solvent mixture. As mentioned above, various batches of

fluorescently labeled PMMA were used. No significant differences were seen between the batches. Table I presents the results of the phase behavior and conductivity measurements we carried out. In experiment (1),<sup>10</sup> we found a constant colloid charge as a function of volume fraction. Experiment (2), the dispersion displaying reentrant melting, forms the subject of this paper, and here we used a different batch of CHB solvent (B). Further experiments were carried out with a third solvent batch, C, which was washed only (Table I). In this case, “normal” phase behavior was observed, i.e., there was no reentrant melting [experiment (3)]. When more ions were introduced to the solvent C by addition of tetrabutyl ammonium bromide salt (TBAB), we again saw reentrant melting [experiment (4)].

Recent work<sup>38</sup> shows that HBr is present due to decomposition of the CHB solvent and suggests that the colloids acquire their charge by *adsorption* of  $H^+$  ions. In the case of experiment (1), the relatively high conductivity suggests that an excess of  $H^+$  was present at colloid volume fractions up to 0.2 at least, and that the colloids could acquire a charge of several hundred elementary charges without significantly altering the overall ionic concentration. Here we expect that both colloid charge and Debye length stay fairly constant as a function of colloid volume fraction. The phase behavior would then be consistent with a Yukawa interaction with a single set of parameters, as we indeed found.

For experiments (2)–(4) the conductivity was much lower and therefore the ion concentration may be strongly affected by the adsorption of ions by the colloids and even by adsorption on the wall of the capillary. We used the conductivity measurements to calculate the ionic strength in the solvent mixture before and after adding colloids, using Walden’s rule. This assumes that the product of the limiting molar conductance,  $\Lambda_0$ , and the viscosity is equal in two solvents. The limiting molar conductance in the solvent of interest is then the product of the ratio of the two viscosities and  $\Lambda_0$  of the reference solvent (which is known). We used literature values for the limiting molar conductance in ethanol of  $53.6 \text{ cm}^2 \text{ S Mol}^{-1}$  for  $H^+$  and  $35.3 \text{ cm}^2 \text{ S Mol}^{-1}$  for  $Br^-$  and used Walden’s rule to determine values of  $18.5 \text{ cm}^2 \text{ S Mol}^{-1}$  for  $Br^-$ ,  $28.1 \text{ cm}^2 \text{ S Mol}^{-1}$  for  $H^+$  and  $4.4 \text{ cm}^2 \text{ S Mol}^{-1}$  for TBAB in CHB decalin. We then assumed that the conductivity of the solvent was equal to the product of the ion concentrations and their limiting molar conductances. The contribution of the large, weakly charged colloids to the conductivity is very small and therefore ne-

TABLE I. Phase behavior using different batches of the CHB solvent component and after addition of TBAB. See text for the ionic strengths in the case of added salt. Note that in the case of CHB A, the conductivity was measured for pure CHB, rather than the CHB-decalin mixture.

Experiment	CHB component of solvent	Freezing	Reentrant melting	Solvent conductivity (pS/cm)	Solvent+ $\eta=0.03$ colloids conductivity (pS/cm)	Solvent treatment	Ionic strength (M)
(1)	CHB A	F-FCC $\eta=0.1$	None	2000 <sup>a</sup>	...	Washed+distilled	$4.3 \times 10^{-8}$
(2)	CHB B	F-BCC $\eta=0.04$	BCC-F, $\eta=0.11$	$190 \pm 30$	$70 \pm 5$	Washed+distilled	$4.3 \times 10^{-9}$
(3)	CHB C	F-BCC $\eta=0.04$	None	$40 \pm 5$	$55 \pm 5$	Washed	$9.8 \times 10^{-10}$
(4)	CHB C+ TBAB salt	F-BCC $\eta=0.04$	BCC-F $\eta=0.13$	$190 \pm 5$	$115 \pm 10$	Washed	

<sup>a</sup>Measured for pure CHB, not mixture of CHB decalin.

glected. In this way, taking measured values of the conductivity, we calculated the ionic strengths of the solvents Table I.

In the case of the batch *B* CHB [experiment (2), Table I] we found that, upon adding colloids, the conductivity was reduced by a factor of approximately four (Table I). We regard this as evidence in favor of ion adsorption by the colloids. In fact, the addition of a colloid volume fraction  $\eta = 0.03$ , with each particle adsorbing several hundred protons would account for almost all the  $H^+$  ions, and result in a fall in conductivity comparable to that which we measured. At higher colloid concentrations we expect that there are insufficient protons, so the charge per colloid is reduced, leading to the reentrant melting behavior observed, as we concluded from our analysis of the confocal microscopy data. The same reasoning can explain experiment (4) in which we were able to induce reentrant melting by adding a small amount of TBAB salt to the solvent. Although larger quantities of TBAB are known to induce inversion of the colloid charge,<sup>39</sup> such that the particles carry a negative charge, this does not occur until a TBAB concentration at least a hundred times higher than the 290 nMol added here. This concentration of TBAB gave a conductivity of 190 pS/cm, similar to that of the batch *B* solvent which exhibited reentrant melting. As in the case of experiment (2), the adsorption of  $H^+$  and, here,  $TBA^+$  and most likely some  $Br^-$ , reduces the calculated ionic strength and hence the conductivity, to an extent similar to that which we measured. However, the magnitude of the measured fall in conductivity is less in the case of experiment (4) than experiment (2), which may reflect the adsorption of the less mobile  $TBA^+$  ions, instead of the faster protons [experiment (2)]. This reasoning does not explain experiment (3). In this case, the conductivity measurements suggest that the maximum number of ions available for each colloid is too low for crystallization to occur at all, according to equation (1). However, assuming the colloids did indeed absorb the available  $H^+$  and (less)  $Br^-$  ions, we expect a 20-fold decrease in ionic strength, and a Debye length of some 4–5  $\mu\text{m}$ , around four times longer than experiment (2) studied in this paper. For this extremely long Debye length the screening of the colloid charge is very limited indeed and may lead to deviations from the behavior predicted by equation (1), possibly resulting in crystallization at lower volume fractions. While a full analysis goes beyond the scope of this work, preliminary comparisons between the primitive model and the Yukawa potential suggest that the Yukawa potential does indeed underestimate the structure in this parameter range, as noted in the nonlinear Poisson-Boltzmann simulations.<sup>9</sup>

## VI. CONCLUSIONS

We have presented results on a model system of charged colloids, which exhibits the unusual phase behavior of reentrant melting and freezing. Strong evidence for the fact that nonpairwise additivity is *not* important here is given by the agreement of the simulations using the Yukawa potential and the primitive model. Instead, by analyzing our experimentally determined radial distribution functions and the particle

excursions in the BCC crystal, we find that the colloid charge falls as a function of volume fraction, which can explain the observed phase behavior. At colloid volume fractions above a few percent, we believe there are insufficient positive ions per colloid, leading to a fall in colloid charge with volume fraction, and the reentrant phase behavior we observed. The second freezing transition at  $\eta \approx 0.5$  is attributed predominantly to hard-core interactions. The high volume fraction crystal has a different symmetry (RHCP) to the BCC crystal formed at lower colloid volume fractions. Finally, we note that it is dangerous to consider only freezing at higher volume fractions and assume from this that a colloidal system has hard-sphere-like behavior. It is clear that, as shown for the present system, the interactions at lower volume fractions should be characterized as well, and may depend strongly on volume fraction.

## ACKNOWLEDGMENTS

The primitive model code is based on that of Athanasios Panagiotopoulos. It is a pleasure to thank Paul Bartlett, Maarten Biesheuvel, Jan Groenewold, Hans-Hennig von Grünberg, Robert Hoy, J. Hans Lyklema, Willem Kegel, Vladimir Lobaskin, Hartmut Löwen, Thomas Palberg, and René van Roij for helpful comments. Willem Kegel and René van Roij are also thanked for a critical reading of the manuscript. Didi Derks is thanked for particle synthesis and solvent purification. This work is part of the Stichting voor Fundamenteel Onderzoek der Materie (FOM), which is supported by Nederlandse Organisatie voor Wetenschappelijk Onderzoek (NWO).

- <sup>1</sup>W. K. Lee, B. A. Wintner, E. Fontes, P. A. Heiney, M. Ohba, J. N. Hasettine, and A. B. Smith III, *Liq. Cryst.* **4**, 87 (1989).
- <sup>2</sup>G. A. McConnell and A. P. Gast, *Macromolecules* **30**, 435 (1997).
- <sup>3</sup>A. C. Anderson, W. Reese, and J. C. Wheatley, *Phys. Rev.* **130**, 1644 (1963).
- <sup>4</sup>P. N. Pusey and W. van Megen, *Nature (London)* **320**, 340 (1986); P. G. Bolhuis, D. Frenkel, S.-C. Muse, and D. A. Huse, *ibid.* **388**, 235 (1997), and references therein.
- <sup>5</sup>W. B. Russel, D. A. Saville, and W. R. Schowalter, *Colloidal Dispersions* (Cambridge University Press, Cambridge, UK, 1989).
- <sup>6</sup>A. van Blaaderen and P. Wiltzius, *Science* **270**, 1177 (1995).
- <sup>7</sup>E. J. W. Verwey and J. Th. G. Overbeek, *Theory of the Stability of Lyophobic Colloids* (Elsevier, New York, 1948).
- <sup>8</sup>S. Alexander, P. M. Chaikin, P. Grant, G. J. Morales, P. Pincus, and D. Hone, *J. Chem. Phys.* **80**, 5776 (1984).
- <sup>9</sup>H. Löwen and G. Kramposthuber, *Europhys. Lett.* **23**, 673 (1993).
- <sup>10</sup>C. P. Royall, M. E. Leunissen, and A. van Blaaderen, *J. Phys.: Condens. Matter* **15**, S3581 (2003).
- <sup>11</sup>E. Trizac, L. Bocquet, and M. Aubouy, *Phys. Rev. Lett.* **89**, 243801 (2002); E. Trizac and Y. Levin, *Phys. Rev. E* **69**, 031403 (2004).
- <sup>12</sup>Y. Monovoukas and A. P. Gast, *J. Colloid Interface Sci.* **128**, 533 (1989).
- <sup>13</sup>J. Yamanaka, H. Yoshida, T. Koga, N. Ise, and T. Hashimoto, *Phys. Rev. Lett.* **80**, 5806 (1998); A. Toyotama, A. Toyotama, T. Sawada, J. Yamanaka, and K. Kitamura, *Langmuir* **19**, 3236 (2003).
- <sup>14</sup>L. F. Rojas, C. Urban, P. Schurtenberger, T. Gislser, and H. H. von Grunberg, *Europhys. Lett.* **60**, 802 (2002); M. Dijkstra and R. van Roij, *J. Phys.: Condens. Matter* **10**, 1219 (1998).
- <sup>15</sup>M. Brunner, C. Bechinger, U. Herz, and H. H. von Grunenberg, *Europhys. Lett.* **58**, 926 (2002).
- <sup>16</sup>C. Russ, H. H. von Grunberg, M. Dijkstra, and R. van Roij, *Phys. Rev. E* **66**, 011402 (2002); A.-P. Hynninen, M. Dijkstra, and R. van Roij, *J.*

- Phys.: Condens. Matter **15**, S3549 (2003); Phys. Rev. E **69**, 061407 (2004).
- <sup>17</sup>R. van Roij and J.-P. Hansen, Phys. Rev. Lett. **79**, 3082 (1997); R. van Roij, M. Dijkstra, and J.-P. Hansen, Phys. Rev. E **59**, 2010 (1999).
- <sup>18</sup>J. Baumgartl and C. Bechinger, Europhys. Lett. **71**, 487 (2005).
- <sup>19</sup>A. E. Larsen and D. G. Grier, Nature (London) **385**, 230 (1997).
- <sup>20</sup>B. V. R. Tata, M. Rajalakshmi, and A. K. Arora, Phys. Rev. Lett. **69**, 3778 (1992); T. Palberg and M. Wirth, *ibid.* **72**, 786 (1994); B. V. R. Tata and A. K. Arora, *ibid.* **72**, 787 (1994).
- <sup>21</sup>J. Ray and G. S. Manning, Langmuir **10**, 2450 (1994); P. Linse and V. Lobaskin, J. Chem. Phys. **112**, 3917 (2000); Phys. Rev. Lett. **83**, 4208 (1999).
- <sup>22</sup>A. Z. Panagiotopoulos and S. K. Kumar, Phys. Rev. Lett. **83**, 2981 (1999).
- <sup>23</sup>A.-P. Hynninen, M. Dijkstra, and A. Z. Panagiotopoulos, J. Chem. Phys. (submitted).
- <sup>24</sup>A. Yethiraj and A. van Blaaderen, Nature (London) **421**, 513 (2003).
- <sup>25</sup>G. Bosma, C. Pathmanoharan, E. H. A. de Hoog, W. K. Kegel, A. van Blaaderen, H. N. W. Lekkerkerker, J. Colloid Interface Sci. **245**, 292 (2002).
- <sup>26</sup>A. D. Hollingsworth and D. A. Saville, J. Colloid Interface Sci. **257**, 65 (2003).
- <sup>27</sup>R. Piazza, T. Bellini, and V. Degeorgio, Phys. Rev. Lett. **71**, 4267 (1993); R. van Roij, J. Phys.: Condens. Matter **15**, S3569 (2003); M. Rasa and A. P. Philipse, Nature (London) **429**, 857 (2004).
- <sup>28</sup>C. P. Royall, R. van Roij, and A. Van Blaaderen, J. Phys.: Condens. Matter **17**, 2315 (2005).
- <sup>29</sup>R. Hunter, *Zeta Potential in Colloid Science* (Academic, New York, 1981).
- <sup>30</sup>R. L. Henderson, Phys. Lett. A **49**, 197 (1974).
- <sup>31</sup>N. G. Almarza and E. Lomba, Phys. Rev. E **68**, 011202 (2003).
- <sup>32</sup>D. Frenkel and B. Smit, *Understanding Molecular Simulation*, 2nd ed. (Academic, San Diego, 2002).
- <sup>33</sup>J. A. Weiss, A. E. Larsen, and D. G. Grier, J. Chem. Phys. **109**, 8659 (1998).
- <sup>34</sup>A.-P. Hynninen and M. Dijkstra, Phys. Rev. E **68**, 021407 (2003).
- <sup>35</sup>J. P. Hansen and I. R. McDonald, *Theory of Simple Liquids*, 1st ed. (Academic, London, 1976).
- <sup>36</sup>M. O. Robbins, K. Kremer, and G. S. Grest, J. Chem. Phys. **88**, 3286 (1988).
- <sup>37</sup>S. Hamaguchi, R. T. Farouki, and D. H. E. Dubin, Phys. Rev. E **56**, 4671 (1997).
- <sup>38</sup>A. D. Hollingsworth, M. E. Leunissen, A. Yethiraj, A. van Blaaderen, P. M. Chaikin, and W. B. Russel (unpublished).
- <sup>39</sup>M. E. Leunissen, C. G. Christova, A. P. Hynninen, C. P. Royall, A. I. Campbell, A. Imhof, M. Dijkstra, R. van Roij, and A. van Blaaderen, Nature (London) **437**, 235 (2005).